

References

- ¹Oswatitsch, K. and Keune, F., "Ein Aquivalenzsatz für Nicht-tangente Fluge Kleiner Spannweite in Schallnaher Strömung," *Zeitschrift für Flugwissenschaften*, Vol. 3, No. 2, Feb. 1955, pp. 29-46.
- ²Whitcomb, R. T., "A Study of the Zero Lift Design Drag Rise Characteristics of Wing-Body Combinations Near the Speed of Sound," NACA Report 1273, 1952.
- ³Malmuth, N. D., Wu, C. C., and Cole J. D., "Slender Body Theory and Optimization Procedures for Transonic Lifting Wing Bodies," *Journal of Aircraft*, Vol. 21, April 1984, pp. 256-263.
- ⁴Shankar, V., "Numerical Boundary Condition Procedure for the Transonic Axisymmetric Inverse Problem," NASA CP 2201, 1981, pp. 183-197.
- ⁵Chan, Y. Y., Mundie, D. L., and Jones, D. J., "Transonic Axisymmetric Bodies with Minimal Wave Drag," *Canadian Aeronautics and Space Journal*, Vol. 26, No. 3, 1980, pp. 231-234.
- ⁶Hassan, A. A., "A Method for the Design of Shock-Free Slender Bodies of Revolution," *AIAA Journal*, Vol. 24, May 1986, pp. 728-734.
- ⁷Burg, K. and Zierep, J., "Profile Geringsten Widerstandes bei Schallanströmung," *Acta Mechanica*, Vol. 1, 1965, pp. 93-108.
- ⁸Whitcomb, R. T., "Transonic Empirical Configuration Design Process," AGARD-R-712, 1983, pp. 8.1-8.9.
- ⁹Miles, J. W., "On the Sonic Drag of a Slender Body," *Journal of the Aeronautical Sciences*, Vol. 23, Feb. 1956, pp. 146-154.
- ¹⁰Krasnov, N. F., *Aerodynamics of Bodies of Revolution*, edited and annotated by D. N. Morris, American Elsevier, New York, 1970.

Sound Radiation from an Airfoil Encountering an Oblique Gust in Its Plane of Motion

Stewart A. L. Glegg*

Florida Atlantic University, Boca Raton, Florida

I. Introduction

SOUND radiation from airfoils that encounter oblique upwash gusts has been studied extensively, and many formulations²⁻⁴ give the radiated field in terms of the unsteady lift fluctuations resulting from the interaction. When the airfoil encounters a gust in the plane of motion at zero angle of attack, there will be no upwash, and hence no unsteady lift. But, sound radiation will still occur due to the unsteady thickness noise components¹ that radiate sound when a blade of finite thickness encounters a velocity perturbation in the plane of motion. The purpose of this Note is to evaluate the radiated acoustic field and demonstrate its significance. However, the analysis does not include the effect of mean flow distortion on the gust.

The principal application of this analysis is considered to be the prediction of helicopter tail rotor noise. In this case the tail rotor is operating in the wake of the helicopter fuselage and hence, the blades will be moving in and out of the velocity deficit associated with the fuselage wake. This only has velocity components in the direction of flight, and hence the tail rotor will only experience unsteady flow components in the plane of motion.

The analysis is based on the unsteady thickness noise theory described in Ref. 1, and, as will be shown below, the sound radiation is dominated by the transient effect of the blade tip moving into the velocity deficit. Consequently, the effects of blade rotation are not important, and acoustic field can be ob-

tained by considering a simplified model of a semi-infinite blade moving in rectilinear motion into the deficit (see Fig. 1). To apply the results to a helicopter tail rotor, the acoustic pulses generated by the blade tip moving in and out of the deficit are then summed at the correct retarded times and radiation angles relative to the observer.

II. Analysis

Consider an airfoil of semi-infinite span moving in rectilinear motion with velocity U , as illustrated in Fig. 1. The airfoil is initially assumed to be moving through a stationary fluid, before crossing a boundary into a region where the fluid is moving with velocity ΔV parallel to the boundary in the plane of motion. A set of blade-based coordinates y_1 are specified where y_1 lies in the chordwise direction and y_2 in the spanwise direction. The boundary of the moving fluid makes an angle θ with the direction of blade motion. Finally, the observer position is specified in a set of stationary coordinates x_i that are aligned with the moving coordinates when source time τ is equal to zero.

The unsteady thickness noise generated by the interaction of the airfoil with the gust is given¹ by

$$p(x_i, t) = \frac{1}{4\pi} \frac{\partial^2}{\partial t \partial x_\beta} \int_{\Sigma} \left[\frac{\rho_0 h w_\beta}{r |1 - M_r|} \right] d\Sigma \quad \beta = 1, 2 \quad (1)$$

where h is the thickness distribution, w_β the unsteady velocity components in the plane of motion, and Σ the blade planform. The rest of the notation is the same as in Ref. 1.

It is convenient to introduce another set of coordinates (α, ζ, κ) , where α lies normal to the boundary of the moving fluid and ζ lies parallel to the boundary. Then the in-plane gust can be specified as

$$w_\beta = -\Delta V_\beta H(\alpha) \quad \beta = 1, 2$$

where $\Delta V_1 = \Delta V \cos \theta$ and $\Delta V_2 = \Delta V \sin \theta$, and $H(\alpha)$ is the Heaviside function, equal to zero when $\alpha < 0$ and unity when $\alpha > 0$. The α coordinate can be related to the blade-based coordinates y_i through

$$\alpha = y_2 \cos \theta - (y_1 - U\tau) \sin \theta$$

where τ is source time and is related to observer time t using the far-field approximation

$$\tau = [t - (r_0/c_0 - x_i y_i / r_0 c_0)] (1 - M_r)^{-1}$$

and $r_0 = |x_i|$. Hence, α may be redefined in terms of observer time as

$$\alpha = y_2 (\cos \theta + \gamma \sin \theta) - y_1 \sin \theta / (1 - M_r) + U \tau_0 \sin \theta$$

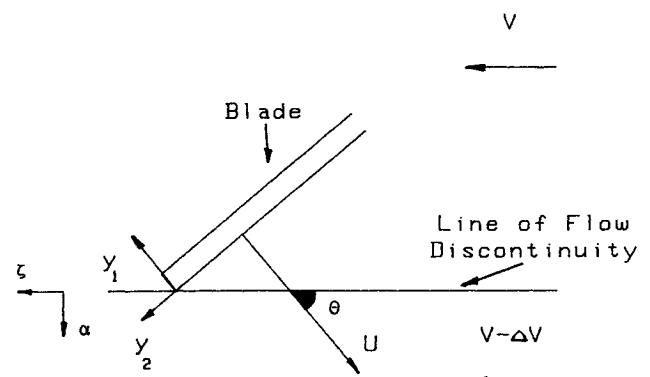


Fig. 1 Semi-infinite blade moving over a boundary separating two flows moving at different velocities. The deficit in the flow velocity is ΔV and the blade velocity is U .

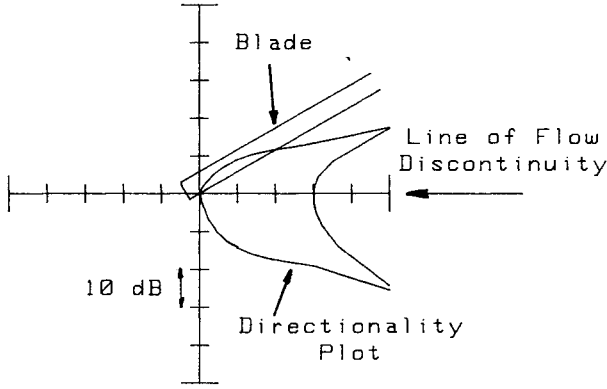


Fig. 2 Directionality plot of the sound pulse generated by a blade encountering a velocity deficit. Angle of blade to boundary is 60 deg.

where

$$\tau_0 = (t - r_0/c_0) \cdot (1 - M_r)^{-1} \text{ and } \gamma = \frac{Mx_2}{r_0(1 - M_r)}$$

Using these definitions, Eq. (1) can be rewritten, for a semi-infinite, untapered blade with a thickness distribution $h(y_1)$ as

$$p(x_i, t) = \left\{ \frac{x_\beta \rho_0 \Delta V_\beta}{4\pi r_0^2 |1 - M_r| c_0} \right\} \frac{\partial^2}{\partial t^2} \times \int_0^c \int_{-\infty}^{\infty} h(y_1) H(-y_2) H(\alpha) dy_1 dy_2$$

Then, by evaluating

$$\frac{\partial H(\alpha)}{\partial t} = \frac{U \sin \Theta}{(1 - M_r)} \delta(\alpha)$$

where $\delta(\alpha)$ is a Dirac delta function, the integral over y_2 can be evaluated given

$$p(x_i, t) = \left\{ \frac{x_\beta \rho_0 \Delta V_\beta}{4\pi r_0^2 |1 - M_r| c_0} \right\} \frac{\partial}{\partial t} \times \int_0^c h(y_1) H(-y_2^*) \frac{U \sin \Theta}{|\alpha'| (1 - M_r)} dy_1$$

where

$$\alpha' = \partial \alpha / \partial y_2 = \cos \Theta + \gamma \sin \Theta$$

and

$$y_2^* = [y_1 (1 - M_r)^{-1} - U \tau_0] \frac{\sin \Theta}{\alpha'}$$

Next we evaluate

$$\frac{\partial H}{\partial t}(-y_2^*) = \frac{U \sin \Theta}{\alpha' (1 - M_r)} \delta(-y_2^*)$$

and integrate over y_1 to obtain

$$p(x_i, t) = \left\{ \frac{-x_\beta \rho_0 \Delta V_\beta U^2}{4\pi r_0^2 (1 - M_r)^2 c_0} \right\} \frac{h(U \tau^*)}{(\cot \Theta + \gamma)} \quad 0 < \Theta < \pi \quad (2)$$

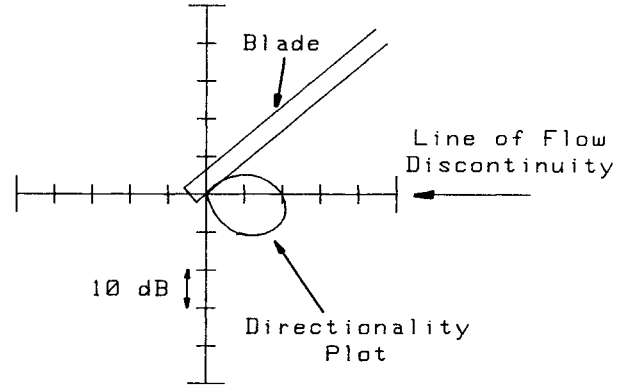


Fig. 3 Directionality plot of the sound pulse generated by a blade encountering a velocity deficit. Angle of blade to boundary is 50 deg.

where

$$\tau^* = t - r_0/c_0$$

This is the principal result of this Note and it demonstrates that as the airfoil moves into the moving fluid a pressure pulse is emitted whose shape corresponds to thickness distribution h and has a timescale of c/U . For example, if the airfoil had a triangular thickness distribution, the acoustic pulse would also be triangular and would occur during the interval $0 < t - r_0/c_0 < U/c$. It is noteworthy that it is the discontinuity at the tip of the blade that generates this pulse. The interesting feature however, is the directionality controlled by

$$\frac{x_\beta \Delta V_\beta}{\Delta V r_0 (\cot \Theta + \gamma) (1 - M_r)^2}$$

This becomes infinite when $\cot \Theta + \gamma = 0$, and to explain this feature we note that the leading edge of the blade translates along the boundary with velocity $U \sec \Theta$. When this intersection moves supersonically, a Mach wave is generated. In the far field, the Mach wave propagates on the surface (x_1, x_2) , which is a solution to $\cot \Theta + \gamma = 0$. A typical directionality plot is shown in Fig. 2, for a blade moving at $M = 0.6$ and $\Theta = 0$ deg. This demonstrates that this source is only significant along beams in the Mach wave directions on either side of the boundary, although radiation does occur throughout the forward arc. If the intersection angle is reduced to 50 deg for this blade speed, then the blade no longer moves supersonically along the boundary and a much reduced directionality occurs, as shown in Fig. 3.

III. Conclusions

The sound radiation from a blade encountering a velocity deficit in its plane of motion has been analyzed and it has been shown that significant radiation can occur due to the unsteady thickness noise component. The maximum radiation occurs when the intersection of the leading edge of the blade with the boundary moves supersonically. In this case, high levels occur in the direction of Mach wave propagation.

The sound is generated by the interaction of the blade tip with the boundary, and a pressure pulse is emitted with the shape of the blade thickness distribution, and a timescale that corresponds to the time for the blade tip to move through the boundary. The levels are linearly proportional to the velocity deficit and the thickness of the blade.

The principal application of these results is seen to be to helicopter tail rotors that operate in the fuselage wake and may encounter velocity deficits of this type. The radiation levels are very dependent on the intersection angle of the blades with the flow boundary and have a strongly directional

character. For this reason this source is only likely to be identified experimentally in static tests when microphones are placed close to the appropriate Mach wave propagation angle. However, on a flyer there will be a period when the levels on the flight path may be dominated by this type of highly directional source.

Acknowledgment

This work was supported by Nasa Research Grant NAG-1-715. The author would like to thank Dr. F. Farassat for his assistance.

References

- ¹Glegg, S., "Significance of Unsteady Thickness Noise," *AIAA Journal*, Vol. 23, 1987, pp. 839-844.
- ²Amiet, R. K., "Acoustic Radiation from an Airfoil in a Turbulent Stream," *Journal of Sound and Vibration*, Vol. 41, 1975, pp. 407-420.
- ³Mugridge, B. D. and Morfey, C. L., "Sources of Noise in Axial Flow Fans," *Journal of the Acoustical Society of America*, Vol. 51, 1972, pp. 1411-1426.
- ⁴Sevik, M., "Sound Radiation from a Subsonic Rotor Subjected to Turbulence," NASA SO-304, Part II, 1970.

Spectral Measurements of Pressure Fluctuations on Riblets

W. L. Keith*

Naval Underwater Systems Center,
New London, Connecticut

Introduction and Experimental Apparatus

A RECENT summary of riblet research is given by Wilkinson et al.¹ of NASA Langley. The authors state, "Of all the nonplanar surface approaches to turbulent viscous drag reduction, riblets are the best established, with little, if any, remaining doubt regarding their effectiveness. The main thrust of the initial Langley riblet research was to verify riblet drag reduction and optimize its level. This effort culminated in the selection of a symmetrical V-groove as the optimal design ($h^+ = S^+ = 15.8$ percent drag reduction)." The investigation reported here was aimed at determining if any measurable changes are induced by riblets in the autospectral density, the streamwise cross-spectral density, and the convection velocity of the fluctuating wall pressure field. Due to the attenuation resulting from spatial averaging, only scales associated with the outer region of the turbulent boundary layer were resolved.

The experiments were conducted in the rectangular test section of the quiet water tunnel at the Naval Underwater Systems Center, New London Laboratory. The water tunnel is a recirculating flow facility, with acoustic isolation provided by rubber hoses between the test section, plenum chambers, and centrifugal pump. The interior of the test section is 83 in. long, 12 in. wide, and increases in height linearly from 4 in. at the inlet to 4.41 in. at the exit, resulting in a zero pressure gradient flow to within ± 0.005 psi. Two piezoelectric pressure transducers fabricated of PZT-5H Type 2 material, of diameter

0.08 in., were flush mounted in the bottom wall, with a streamwise separation of 0.4 in. center to center. The output voltage signals were amplified 20 dB by an Ithaco Model 143N preamplifier, an additional 20 dB by an Ithaco Model 455 amplifier with an adjustable high pass filter (set at 1 Hz), and were then input to a Spectral Dynamics Model SD375 spectrum analyzer. All of the spectra were computed from 500 ensemble averages. Measurements of the mean streamwise velocity $u(y)$ were made using a TSI model 9100 laser Doppler velocimetry system. The riblet coating, which was identical to that used on the yacht "Stars and Stripes," was manufactured by the Scotch 3M Corporation. The symmetrical V-grooves had height (h) and peak-to-peak spacings (S) of 0.0045 in., and a base thickness of 0.0025 in. Following the baseline measurements, the entire bottom wall of the rectangular test section was covered with one continuous layer of riblet material. The riblets extended a distance upstream approximately 60δ from the measurement location.

Experimental Results

The turbulent boundary-layer mean velocity profiles were measured at a streamwise location coincident with that of the pressure transducers, 61.4 in. from the test section inlet and 6 in. from each side wall. The displacement thickness δ^* and momentum thickness θ , determined by numerical integration, are given in Table 1. Based on the R_θ values and velocity profiles, a fully developed turbulent boundary layer existed at both Reynolds numbers. The turbulence intensity in the free-stream was 1.5%. In order to determine the mean wall shear stress τ_w , the boundary-layer profiles and static pressures were measured at streamwise locations along the test section. Values for τ_w were then determined from a momentum balance analysis. The velocity defect $[(U_\infty - u(y))/u^*]$ was plotted for both Reynolds numbers investigated and was found to agree well with Hama's² empirical expression for zero pressure gradient flat-plate turbulent boundary layers, given as $9.6(1 - y/\delta)^2$. The nondimensional scales of the riblets S^+ and pressure transducers d^+ are given in Table 1. The freestream velocity of 10 ft/s provided an optimum turbulent boundary layer for the performance of the riblets, based on the results of Wilkinson et al.¹

Corcos³ derived a method to correct autospectra for the attenuation due to spatial averaging associated with circular-faced transducers. The baseline measurements of the corrected autospectral density $\Phi(\omega)$ nondimensionalized on outer flow variables δ^* and U_∞ are presented in Fig. 1. Also shown are the

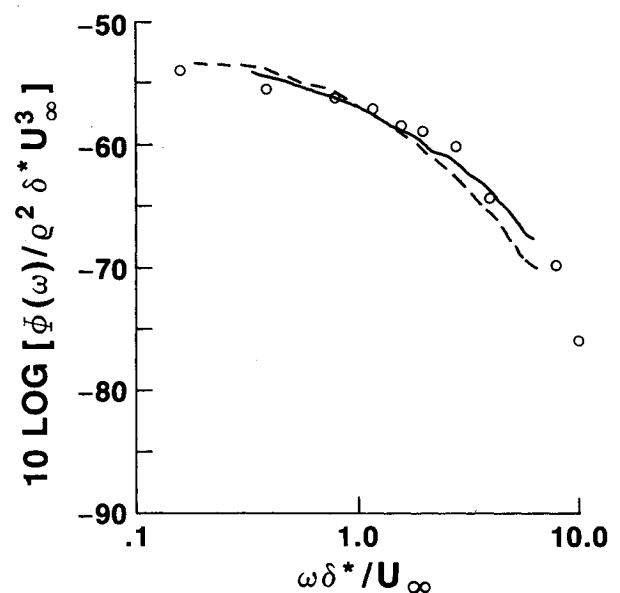


Fig. 1 Nondimensional autospectra $\Phi(\omega)/\rho^2 \delta^* U_\infty^3$. Corrected for spatial averaging, — $U_\infty = 10$ (ft/s), --- $U_\infty = 20$ (ft/s), \circ = results of Bakewell et al.⁴